Polymer Vol. 37 No. 4, pp. 687–698, 1996

0032-3861/96/$15.00 + 0.00

Preparation and properties of comb-like polymers obtained by radical homo- and copolymerization of a liposaccharidic monomer with styrene

Javier Revilla, T. Delair and Christian Pichot*
UMR 103 CNRS-bioMérieux, 46 allée d'Italie, 69007 Lyon, France

and Bernard Gallot
Laboratoire des Matériaux Organiques à Propriétés Spécifiques, CNRS, BP 24, 69390 Vernaison, France
(Received 8 January 1995; revised 7 June 1995)

A new disaccharide polymerizable surfactant 11-(*N*-*p*-vinyl benzyl) amidoundecanoyl maltobionamide (LIMA, **6**), was synthesized through a five-step procedure. It was found to exhibit a Krafft point of 52°C and a critical micelle concentration of 1.2×10^{-3} mol l^{-1} at 55 C (as measured by surface tension and fluorescence techniques). Radical-initiated homo- and copolymerization of LIMA (M) with styrene (S) have been performed at 60°C in deuterated dimethyl sulfoxide using 2,2′-azobisisobutyronitrile as initiator. Kinetics were followed both by ^{1}H n.m.r. and gas chromatography analyses providing $k_p/k_t^{1/2}$ value for LIMA homopolymerization and a set of reactivity ratios such as: $r_M = 0.86 \pm 0.1$ and $r_S = 1.23 \pm 0.09$. Homopoly(LIMA) and copolymers with styrene were characterized as regards to average composition and molecular weight. Comb-like polymers were examined by X-ray analysis in the solid state; they were found to exhibit lamellar liquid-crystalline structures (smectic) resulting from the superposition of hydrophilic and hydrophobic layers.

(Keywords: lipomaltobionamide; surface activity; radical copolymers)

INTRODUCTION

In recent years, the development of carbohydrate-containing polymeric materials has received increasing attention because of practical and academic interests. One potential advantage of polysaccharides is their ability to covalently bind biological molecules via oxidation of the numerous alcohol functions and, in addition, their hydrophilic nature prevents non-specific adsorption and denaturation of proteins. As a result, many synthetic polymers with pendant saccharidic residues were prepared which were found quite attractive in many biological applications such as cell-specific biomedical materials[1–6], pharmacological substances[7–9], and tools for investigating biological recognition phenomena[10–14].

A great deal of effort has been devoted to the synthesis of carbohydrate monomers for various applications[15] and which have been categorized according to the type of linking between the polymerizable group and the saccharidic moiety: ester, ether, amide, glycosidic. Recently, special emphasis was directed towards the preparation of saccharidic monomers showing amphiphilic structures and various synthesis strategies with different carbohydrates were performed for making monomers with variable hydrophilic–lipophilic balance. The resulting comb-like homo- or copolymers were found to exhibit outstanding properties, especially a liquid-crystal behavior under solid state. This was well illustrated in the case of polymers prepared from acrylamido-*N*-alkyl glucamines[16], alkyl methacrylate-terminated glucosides[17], and alkylglucosides[18].

To date, few kinetic studies have been reported on the radical-initiated polymerization behavior of such carbohydrate-containing amphiphilic monomers, which could be particularly useful for better control of the composition and as well for determining the microstructure before manufacturing copolymers for further examination of specific properties. In this respect, a recent study of this laboratory[19] was devoted to the synthesis of various surface-active cellobiose monomers using the glycosylation reaction for introducing a spacer arm onto the anomeric center. An hexylmethacrylate derivative was especially designed and it was proved to fairly homopolymerize in solution conditions and in addition, copolymerization reactivity ratios with styrene were determined. The resulting copolymers were found to exhibit liquid-crystal behaviour in the solid state, even when swollen with water[20]. Moreover, it has been surface polymerized onto latex particles with a relatively good yield allowing the preparation of hydrophobic supports

* To whom correspondence should be addressed

with immobilized sugar moieties[21]. This surface-active property of a carbohydrate–amphiphile was recently confirmed by Demharter *et al.*[22] who synthesized and used a *N*-methyl-*N*-(11-(acryloyamino)-undecanoyl)glucamine in the batch emulsion polymerization of styrene giving monodisperse particles with saccharidic modified surfaces.

Based on the performance acquired with the cellobiose derivative, the synthesis of a new amphiphilic monomer bearing a pendant saccharidic moiety was conceived with the following strategy:

—to use a styrenic group as a polymerizable function in order to favour the preparation of styrene copolymers with homogeneous compositions as well as the incorporation of the amphiphile onto polystyrene-based particles.

—to impart a spacer long enough to separate the hydrophilic part from the main chain and attached to the styrenic group through a stable amide linkage.

—to bind a saccharidic moiety derived from available carbohydrate molecules (such as maltose, for instance) to the end of the linker and with a structure allowing significant enhancement of the hydrophilic–lipophilic balance suitable for immobilizing biologically-active molecules.

The first part of this paper reports on the synthesis and characterization of this surface-active saccharadic monomer, 11-(*N*-*p*-vinylbenzyl) amidoundecanoyl maltobionamide. The second part deals with the study of radical-initiated homopolymerization and copolymerization of this monomer with styrene under solution conditions in order to determine several pertinent kinetic parameters. Finally, some molecular properties of the corresponding polymers were characterized, such as molecular weight and distribution and copolymer composition; in addition, their liquid-crystal properties have been carefully examined by X-ray analysis.

EXPERIMENTAL

Materials

Dicyclohexylcarbodiimide (DCC), *N*-hydroxsuccinimide (HOSu), and 11-aminoundecanoic acid from Aldrich were used as received. D(+)-Maltose monohydrate was purchased from Fluka. 4,4′-Azobisisobutyronitrile (AIBN, 99% pure from Merck) was recrystallized before use. Styrene monomer (99% pure from Janssen) was purified by vacuum distillation and stored at −20°C until use. Vinylbenzyl chloride (purchased from Dow Chemical) was a mixture of the *meta* (60%) and *para* (40%) isomers. Solvents were purified by classical methods to eliminate oxygen.

Synthesis of the LIMA monomer

*11-*N*-t-butyloxycarbonyl aminoundecanoic acid* (**2**): 20.13 g (100 mmol) of 11-aminoundecanoic acid (**1**) was dissolved in the following mixture: 100 ml 1 N NaOH/100 ml water/100 ml dioxane/100 ml THF, then 21.82 g (100 mmol) of di-t-butyl dicarbonate (diBoc) was added in small amounts and the mixture was stirred overnight at room temperature. THF was evaporated under reduced pressure, the resulting solution was acidified to pH = 1 by 1 N HCl. The precipitate was filtered off and washed 3 times with 50 ml water at pH = 1 and dried under vacuum. Finally, (**2**) was dissolved in acetone and recrystallized in water at pH = 1 (yield 91%).

^{1}H n.m.r. ($CDCl_3$, d ppm): 4.54 (m, 1H), 3.08 (m, 2H), 2.34 (t, 2H, J = 7.4 Hz), 1.62 (m, 2H), 1.44 (s, 11H), 1.28 (s, 12H).

*11-*N*-t-butyloxycarbonyl aminoundecanoyl-succinimidyl ester* (**3**): 27.1 g (90 mmol) of (**2**) was dissolved in THF (200 ml), then 11.75 g (99 mmol) of HOSu and 18.76 g (90 mmol) of DCC were added at 0°C and the solution was stirred for 5 h. After standing overnight at 4°C, the dicyclohexylurea (DCU) precipitate was filtered off and washed with acetone. The excess solvent was eliminated under reduced pressure; (**3**) was precipitated in 1.5 l of water at pH = 7 and dried under vacuum (yield 93%).

^{1}H n.m.r. ($CDCl_3$, d ppm): 4.54 (m, 1H), 3.08 (q, 2H, J = 7.0 Hz), 2.38 (s, 4H), 2.60 (t, 2H, J = 75 Hz), 1.70 (quintuplet, 2H, J = 7.5), 1.44 (s, 11H), 1.28 (s, 12H).

*11-*N*-t-butyloxycarbonyl aminoundecanoyl-aminomethylstyrene* (**4**): 24.75 g (62.2 mmol) of (**3**) and 8.27 g (62.2 mmol) of *p*-vinylbenzylamine (prepared from *p*-vinylbenzyl chloride[23] according to the Gabriel synthesis[24]) were dissolved in THF (450 ml) then 17.5 ml of triethylamine (124 mmol) was added. The mixture was stirred overnight at room temperature and concentrated at 40°C under reduced pressure. The concentrated solution was poured into 700 ml of water at pH = 2 while stirring and the precipitate was filtered off and dried under vacuum (yield 93%).

^{1}H n.m.r. (DMSO-d_6, d ppm): 7.30 (m, 4H), 6.71 (dd, 1H, J_{cis} = 10.9 Hz, J_{trans} = 17.6 Hz), 5.73 (dd, 1H, J_{cis} = 0.9 Hz, J_{trans} = 17.6 Hz), 5.22 (dd, 1H, J_{cis} = 0.9 Hz, J_{trans} = 10.9 Hz), 4.42 (d, 2H, J = 7.5 Hz), 3.08 (q, 2H, J = 7.5 Hz), 2.20 (t, 2H, J = 7.5 Hz), 1.65 (t, 2H, J = 7.5 Hz), 1.44 (s, 11H), 1.28 (s, 12H).

*11-(*N*-p-vinylbenzyl) amidoundecanoylamine* (**5**): 8.32 g (20 mmol) of (**4**) was dissolved in anhydrous dioxane (30 ml) and 50 ml of 4 N HCl in dioxane was added; the mixture was stirred for 1 h and concentrated under reduced pressure. Ethyl ether (200 ml) was added and the precipitate was filtered off, washed with ethyl ether (100 ml) and dried under vacuum. The solid was dissolved in methanol (80 ml) and Amberlite IRA-400 was added in small amounts until complete neutralization. The resin was filtered off, the solvent was evaporated and (**5**) was dried under vacuum (yield 96%).

^{1}H n.m.r. (DMSO-d_6, d ppm): 8.32 (m, 1H), 7.95 (m, 2H), 7.28 (broad, 4H), 6.70 (dd, 1H, J_{cis} = 10.9 Hz, J_{trans} = 17.6 Hz), 5.75 (dd, 1H, J_{cis} = 0.9 Hz, J_{trans} = 17.6 Hz), 5.25 (dd, 1H, J_{cis} = 0.9 Hz, J_{trans} = 10.9 Hz), 4.25 (m, 2H), 2.70 (m, 2H), 2.13 (t, 2H, J = 7.5 Hz), 1.52 (m, 4H), 1.28 (s, 12H).

*11-(*N*-p-vinylbenzyl) amidoundecanoyl maltobionamide* (**6**): 3.40 g of maltonolactone[3] (10 mmol) was dissolved in methanol (100 ml) under reflux in the presence of a small amount of a polymerization inhibitor (2-6-di-*t*-butyl-4-methylphenol, BHT); 3.16 g (10 mmol) of (**5**) in solution in methanol (50 ml) and 10.02 g of triethylamine (100 mmol) were added. The mixture was refluxed for 4 h and cooled to 0°C; (**6**) was recrystallized from methanol (yield 57%).

^{1}H n.m.r. (DMSO-d_6, d ppm): 7.18–7.35 (m, 4H), 6.71 (dd, 1H, J_{cis} = 10.9 Hz, J_{trans} = 17.6 Hz), 5.73 (dd, 1H, J_{cis} = 0.9 Hz, J_{trans} = 17.6 Hz), 5.22 (dd, 1H, J_{cis} = 0.9 Hz, J_{trans} = 10.9 Hz), 4.44 (d, 2H, J = 7.5 Hz), 3.12 (m, 2H),

2.15 (t, 2H, $J = 7.5$ Hz), 1.45 (m, 2H, 1.40 (m, 2H), 1.27 (m, 12H).

^{13}C n.m.r. (DMSO-d_6, d ppm): Primes designate the terminal β-D-galactopyranosyl residue. 172.2 and 171.7 (C=O), 140.0 and 139.5 phenyl (*ipso*), 137.0 and 136.6 (CH=), 136.3 and 135.6 phenyl (*meta* and *para*), 128.5, 127.4, 126.8, 126.0, 124.8, 124.6, phenyl, 114.1 and 113.7 ($=CH_2$), 100.7 ($C^{1'}$), 83.0 (C^4), 73.3, 73.1, 72.3, 72.1, 71.9, 71.6 (the remaining pyranose carbons), 69.9 ($C^{4'}$), 62.6 (C^6), 60.7 ($C^{6'}$), 41.9 (chain-CH_2-CONH), 41.7 (benzyl methylene), 35.3 (CONH-CH_2-chain), 29.2, 28.9, 28.7, 28.6, 2.3, 25.3 (the remaining aliphatic chain).

$CH_{32}H_{52}O_{12}N_2$ (656.77)	C	H	O	N
Calc.	58.5	7.9	29.3	4.3
Found	57.7	8.2	29.8	4.3

Surface-active properties measurement

Two techniques were performed in order to characterize the surface activity of LIMA: surface-tension measurements and fluorescence with a probe.

The surface tension of aqueous solutions was measured as a function of LIMA concentration by using the ring method with a Lauda tensiometer at 55°C. Increments of monomer (**6**) were added and the surface tension was recorded continuously until it reached a constant value. A plot of the surface tension (γ) *versus* the free LIMA monomer concentration in the aqueous phase (C) was obtained (*Figure 2*), which was used to calculate the critical micelle concentration of the LIMA monomer.

The fluorescence emission spectra of pyrene solubilized in aqueous solutions of lipomaltobionamide (LIMA, **6**) were recorded as a function of the LIMA concentration, using a Perkin–Elmer LS-50 spectrophotometer at an excitation wavelength of 339 nm. The change of intensities in the emission spectrum of monomeric pyrene provides an estimate of the polarity sensed by pyrene in its micellar microenvironment.

Solution polymerization

Radical homopolymerizations and copolymerizations with styrene at various initial monomer compositions (*Table 1*) were performed in a three-necked, round-bottomed flask equipped with a magnetic stirrer and nitrogen inlet.

Procedure. The reaction vessel was loaded with solvent (DMSO-d_6) and monomer(s) at a total concentration of 0.5 mol l^{-1}; the mixture was magnetically stirred and degassed under nitrogen for 1 h at room temperature. The mixture was immersed in an oil-bath until the temperature reached 60°C. The initiator AIBN (2 mol% of the monomer), dissolved in DMSO-d_6, was then introduced, and during the whole reaction an inert atmosphere was maintained in the vessel for 24 h at 60°C.

In order to precipitate the formed polymer, the viscous solution was poured into a 20-fold excess of ethyl acetate, and the polymer was isolated and purified by dissolution in methanol and precipitation from acetone.

Kinetic study. Several samples were taken at various reaction times and placed in an ice bath to stop the polymerization. Gas chromatography (g.c.) analyses of styrene were performed with a Perkin-Elmer AutoSystem GC on a HP-20M Carbowax 20M column (30 m × 0.53 × 1.33 mm film thickness) at a temperature of 190°C and using flame ionization detection. For each sample, three injections were carried out and averaged.

The amount of residual styrene was calculated from the monomer and solvent peak areas according to the following formula:

$$[S]_t = \frac{(S \text{ peak area})_t}{(\text{DMSO peak area})_t} \times \frac{(\text{DMSO peak area})_t}{(S \text{ peak area})_0} \times [S]_0$$

The homopolymerization of LIMA was carried out in deuterated DMSO in order to monitor the polymerization reaction by ^{1}H n.mr. analysis: the amount of residual monomer was calculated from the vinylic proton peak area (I_M) compared to the hydroxyl proton (I_{ref}: -OH, $\delta = 5.55$ ppm). The spectra were recorded on a Brüker AC200 apparatus operating at 200 MHz for proton and 50.3 MHz for ^{13}C. DMSO-d_6 and hexamethyl disiloxane (HMDS) were used as the solvent and internal standard, respectively. The following formula was used to calculate the conversion at time t:

$$\text{conversion}(\%) = \frac{\left(\frac{I_M}{I_{ref}}\right)_0 - \left(\frac{I_M}{I_{ref}}\right)_t}{\left(\frac{I_M}{I_{ref}}\right)_0} \times 100$$

For copolymerization reactions of the LIMA–styrene mixtures, the amount of residual monomer was determined as follows, taking into account the spectral region between 5.0 and 7.0 ppm, which corresponds to the vinylic protons of styrene and lipomaltobionamide. Hydroxyl groups of the saccharidic moiety (4.4–5.7 ppm) were evidenced by adding D_2O to the solution of lipomaltobionamide in DMSO-d_6, signals between 4.4 and 5.7 ppm decreased and disappeared, which shows that they correspond to labile protons. (*Figure 1*).

The overall conversions were calculated according to the above formula in which I_M represents the sum of the peak areas corresponding to the vinylic protons of styrene (I_S) and lipomaltonamide (I_L). The monomer mixture compositions were calculated from the integrations of the LIMA (I_L) and styrene (I_S) vinylic protons according to the formula

$$f_M = \frac{I_L}{I_L + I_S}$$

where f_M represents the LIMA mole fraction.

Table 1 Comparison of $(k_p/\sqrt{k_t})$ values for radical-initiated polymerization of LIMA and various styrene-terminated monomers

Monomer	$k_p/\sqrt{k_t}$ ($l^{1/2}$ mol$^{-1/2}$ s$^{-1/2}$)	T (°C)	Reference
Styrene	0.042	60	37
p-Formylstyrene	0.135	60	37
P29H[a]	0.065	60	37
PVA-macromonomer[b]	0.027	60	37
p-Vinylbenzylamine (VBA)	0.025	60	38
VBA derivative (VBAF)[c]	0.086	60	38
LIMA	0.17	60	this work

[a] Methyl 2,2-dimethyl-3-hydroxy-3-(4′vinylphenyl)propanoate
[b] Styrene-terminated silylated poly(vinyl alcohol) macromonomer
[c] *p*-Vinylbenzyl amine trifluoroacetamide

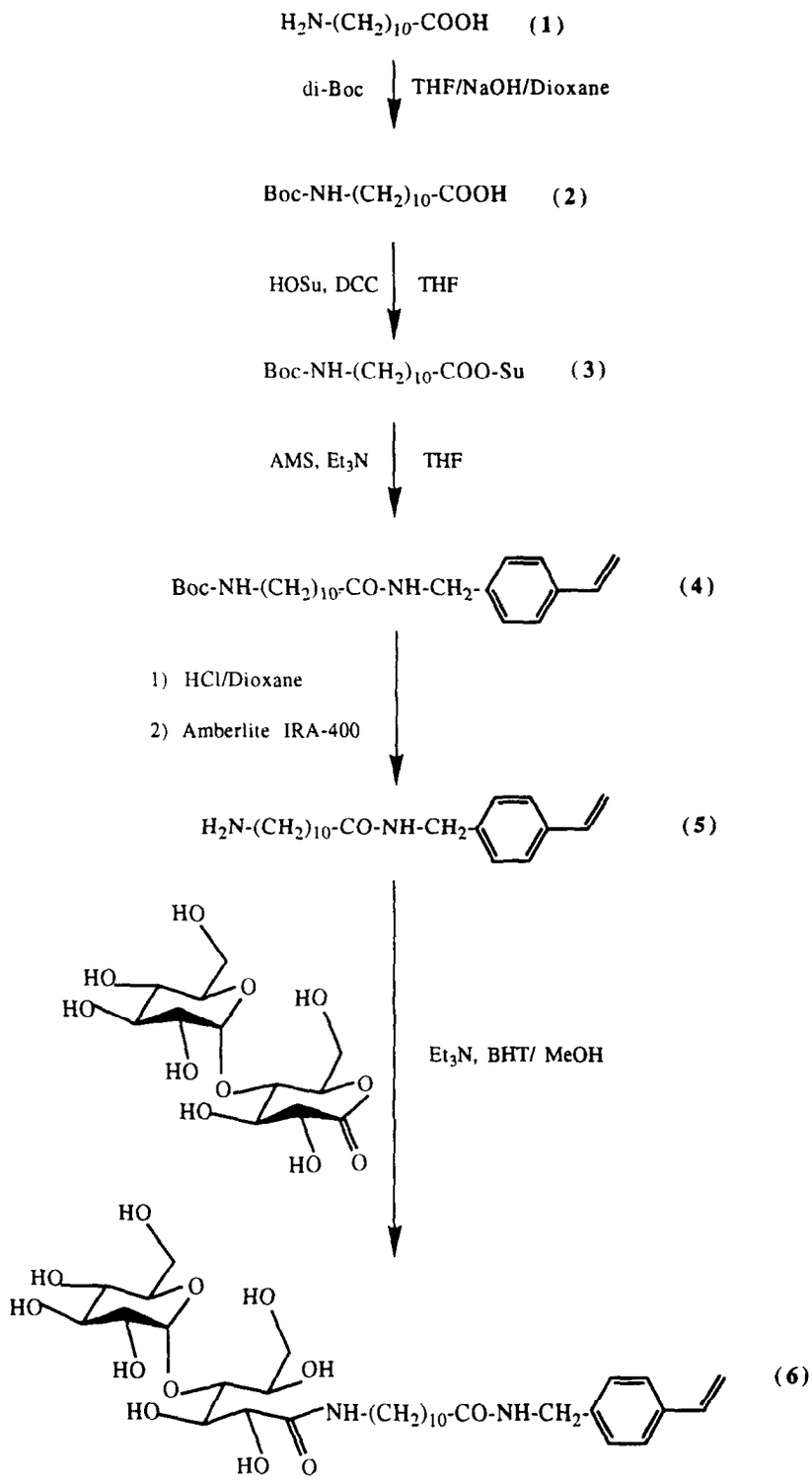

Figure 1 Schematic representation of the various steps for the synthesis of LIMA

From the initial slopes, initial consumption rates R_{Mo} and R_{So} for each monomer were determined, from which the initial copolymer composition could be calculated:

$$F_{Ao} = \frac{d[M]}{d[M] + d[S]} = \frac{R_{Mo}}{R_{Mo} + R_{So}}$$

In the same manner, the total amount of monomer *versus* time gave the initial copolymerization rate R_{po}.

From the initial composition of the monomer mixture (f_{Mo}) for each copolymerization and from the initial instantaneous copolymer compositions (F_{Mo}), reactivity ratios of the system were determined by usual graphic methods: Fineman–Ross[25], Kelen–Tüdos[26], and also a nonlinear estimation method from Tidwell and Mortimer[27].

A simulation program was established, based on the copolymerization equation, giving the monomer feed composition as well as the instantaneous and average copolymer compositions *versus* conversion.

Characterization of (co)polymers (n.m.r., g.p.c.)

The average copolymer composition was determined

from ^{1}H n.m.r. spectra according to the assignments given in *Figure 4*.

If PS = polystyrene and PM = polylipomaltobionamide

aromatic protons $A = 5PS + 4PM$

hydroxyl protons $B = 2PM$

then $PM/(PM + PS) = 5B/(B + 2A)$

= saccharidic mole fraction in the copolymer.

Gel permeation chromatography (g.p.c.) was carried out to characterize the final polymer molecular weight and distribution. A water device was used equipped with a μ-Styragel HT linear 10 mm column and a Shodex KD-802 column. The eluent was DMF at a flow rate of 1.0 ml min^{-1} and detection was performed by measurement of the refractive index (using a differential refractometer Waters 410). Number and weight average molecular weights (M_n and M_w) and polydispersity indexes were derived from a calibration using narrowly distributed polystyrene standards.

X-ray analysis of solid-state polymers

X-ray diffraction experiments were performed on unoriented samples with a Guinier-type focusing camera operating under vacuum equipped with a bent quartz monochromator (reflection 101) giving a linear collimation of strictly monochromatic X-rays (CuKα1, $\lambda = 1.54$ Å) and a device for recording the diffraction patterns from samples at various temperatures between 20°C and 250°C, with an accuracy of ±1°C.

RESULTS AND DISCUSSION

Preparation of the surface-active monomer

The synthesis of the surface-active monomer where the hydrophilic part is constituted of a sugar residue and having a styrene polymerizable group, was performed in five steps. The synthetic route is shown in the scheme depicted in *Figure 1*.

A. *Protection of the α-amine function.* The α-amine function was protected under the form of its *t*-butyloxycarbonyl derivative (**2**) by action of the di-butyl dicarbonate[28,29]. The reaction was carried out in a dioxane/water/1 N NaOH/THF mixture.

B. *Activation of the acid function.* The *N*-protected amino acid (**2**) was actived under the form of its succinimidyl ester (**3**) by an adaption of the method of Paquet[30] using THF as the reaction solvent in the presence of a coupling agent (DCC).

C. *Fixation of the polymerizable group.* The introduction of the polymerizable group was achieved by aminolysis of its active ester end (**3**) by the amine function of aminoethylstyrene and gave the *N*-protected monomer (**4**). One equivalent of aminomethylstyrene was added to the *N*-protected amino acid in THF, in the presence of a twofold excess of triethylamine. The reaction was complete after stirring overnight at room temperature.

D. *Deprotection of the amine function.* The BOC protecting group of (**4**) was removed by the action of hydrogen chloride in dioxane solution and followed by treatment by an anion exchange resin (Amberlite IRA-400) in methanol solution to provide the polymerizable amine (**5**). In order to avoid the presence of polymer, the reaction was performed in anhydrous conditions.

E. *Coupling reaction.* The activated disaccharide (maltonolactone) was condensed with the ω-amine function of the polymerizable amine (**5**) with triethylamine acting as a catalyst and an acid acceptor. In order to avoid spontaneous polymerization, the reaction was performed in the presence of about 1 wt% of inhibitor (BHT). The maltonolactone was prepared by hypoiodite oxidation of maltose according to the method described by Kobayashi[3]. This simple method has several advantages: the yield is high and the oligosaccharide requires no protection of its hydroxyl groups. A white, crystalline compound was finally recovered.

A complete assignment of proton signals of this surface-active monomer (LIMA) in DMSO-d_6 was achieved by 2-dimensional n.m.r. and inspection of the chemical shifts.

Krafft point and critical micelle concentration (CMC) of LIMA

LIMA was found to be very soluble in polar solvents such as DMF and DMSO. On the contrary, solutions of LIMA in water were cloudy at room temperature; after immersion in a thermostated bath and controlled increase of temperature, the aqueous solution became transparent at 52°C which is defined as the Krafft point of the amphiphile.

Figure 2 shows a semi-logarithmic plot of the water–air interface tension as a function of the concentration of LIMA. The concentration at the break-point of the curve corresponds to the CMC and it was found to be equal to 1.2 mmol l^{-1}.

In addition, the effect of the surface-active monomer concentration on the fluorescence of pyrene in water (near saturation, ca. 6×10^{-7} M) was examined.

In the presence of micelles and other macromolecular systems, pyrene is preferentially solubilized in the interior hydrophobic region of these aggregates[31,32]. Below the CMC, no micelles are present and the

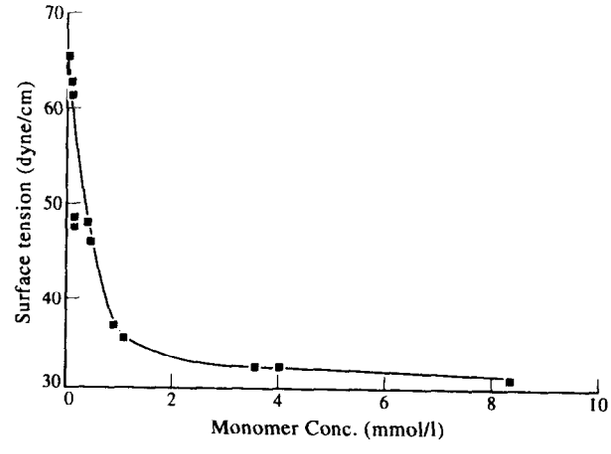

Figure 2 Plot of the water–air surface tension (γ) as a function of LIMA concentration

pyrene fluorescence spectrum corresponds to that in water. Furthermore, as the emulsifier concentration increases above the CMC, pyrene is solubilized in the hydrophobic interior.

Figure 3 shows the variation of the total fluorescence intensity (I) *versus* different concentrations of surface-active monomer in the presence of 6×10^{-7} M pyrene. Below a given concentration (1.3 mmol l^{-1}), I is roughly constant, and above this concentration, the intensity increases with increasing concentrations. This change in intensity reflects the onset of micelle formation and the partitioning of pyrene between the aqueous and micellar phases. The slope change was attributed to the fact that pyrene has a very different lifetime in water than in the micellar phase, as previously reported by Winnik *et al.*[33,34].

There is an excellent agreement between the CMC determined by this method and that deduced from surface-tension measurement, indicating the reliability and complementarity of this technique.

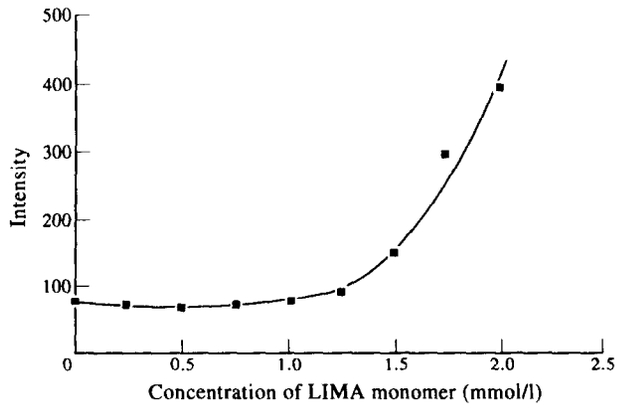

Figure 3 Plot of the total fluorescence intensity for pyrene in water as a function of LIMA concentration

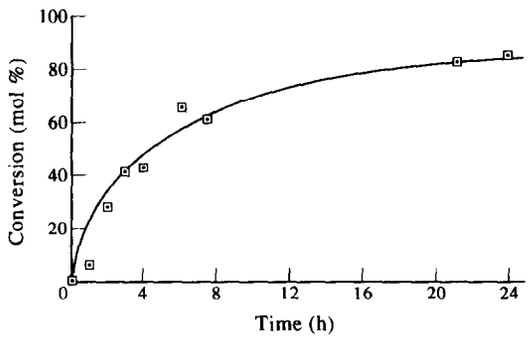

Figure 4 Conversion *versus* time curve (from ^{1}H n.m.r. analysis) for LIMA homopolymerization in DMSO-d_6 solution

Kinetic studies

Homopolymerization of LIMA. The homopolymerization of monomer (6) was carried out in DMSO-d_6 with AIBN (2 mol.% of the monomer) as initiator at 60°C. As previously detailed, the kinetics were followed by ^{1}H n.m.r., which allows quantification of monomer consumption through the decrease of the vinylic proton peak intensity. Kinetic data are reported in *Figure 4*, showing the variation of the conversion *versus* time. These data were used to determine the so-called $k_p/\sqrt{k_t}$ ratio, by combining the general equation for the polymerization rate[35]

$$R_p = \frac{d[M]}{dt} = k_p[M](f \cdot k_a \cdot [I]/k_t)^{1/2}$$

and that related to the rate of decomposition of the initiator $[I] = [I]_o \cdot e^{-k_d \cdot t}$ which leads to

$$\ln \frac{[M]_o}{[M]} = 2\frac{k_p}{\sqrt{k_t}}(f \cdot [I]_o/k_d)^{1/2}(1 - e^{-k_d \cdot t/2})$$

where $[M]_o$ and $[M]$ are monomer concentrations (initial and at time t, mol l^{-1}), k_p and k_t are, respectively, the propagation and termination rate constants (1 mol^{-1} s^{-1}), f is the initiator efficiency, k_d is the initiator decomposition rate constant (s^{-1}), and $[I]_o$ is the initial initiator concentration (mol l^{-1}).

k_d has been reported as 1.34×10^{-5} s^{-1} for AIBN at 60°C in DMSO and the initiator efficiency $f = 0.5$ according to literature values[36]. The $k_p/\sqrt{k_t}$ ratio can be calculated with a good accuracy from the slope of the curve shown in *Figure 5*; the value is reported in *Table 2*, together with those of styrene and styrene derivatives, as obtained under similar conditions in this laboratory[37,38].

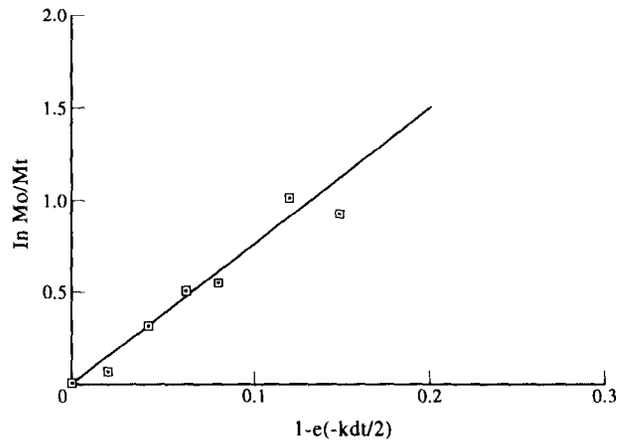

Figure 5 Semi-logarithmic variation of the monomer consumption *versus* the decomposition rate of initiator

Table 2 Kinetic data for the solution copolymerization of LIMA (M) with styrene (S) in DMSO-d_6

Code	$(S)_o$ (mol l^{-1})	$(M)_o$ (mol l^{-1})	$(I)_o$ (mol l^{-1})	$R_{po} \times 10^5$ (mol l^{-1} s^{-1})	f_{Mo}	F_{Mo} Exp.	F_{Mo} Theor.
Homo1	0.500		0.02	3.00			
Copo 5	0.375	0.125	0.02	0.945	0.250	0.170	0.215
Copo 6	0.288	0.250	0.02	1.103	0.465	0.465	0.420
Copo 7	0.230	0.300	0.02	1.140	0.566	0.569	0.522

It is clearly shown that the LIMA monomer exhibits a higher $k_p/\sqrt{k_t}$ value than styrene derivatives. Such an effect is difficult to explain since it can be caused either by a decrease in k_t or an increase in k_p. The former hypothesis might be more realistic since the termination between two hindered macroradicals should be disfavored.

In fact, much work has already been devoted to the chain-length dependence of those reactions, especially in the case of alkyl methacrylates[39–43] and showing a significant increase of $k_p/k_t^{1/2}$ with the length of the alkyl chain. It was particularly demonstrated for MMA and lauryl methacrylate[43] that such an effect originated from a decrease of the termination rate constant. A recent paper from this laboratory[19] also showed a similar effect in the case of the cellobiose monomer (6-(methacryloyloxy)hexyl-D-cellobioside) since a value of 0.20 was obtained for $k_p/k_t^{1/2}$. In addition, the observed decrease of $k_p/k_t^{1/2}$ above 60% conversion for that monomer suggested that the radical polymerization kinetics were diffusion controlled.

In the absence of any data on the absolute kinetic constants for LIMA homopolymerization, it may be assumed that k_t might be also markedly lower than in the case of styrene because of the presence of the bulky amide substituent. Another alternative could also be invoked, which consists of assuming some molecular organization of LIMA in DMSO and favoring the packing of the monomer double bonds. In that case, the propagation rate constant would be obviously enhanced; however, we did not obtain any experimental evidence for such organization.

Reactivity ratios of the styrene–LIMA system. A kinetic study of the copolymerization of LIMA with styrene was carried out under identical experimental conditions. The same ^{1}H n.m.r. analytical procedure as for homopolymerization kinetics was performed in order to access the individual monomer consumptions. The curves of monomer consumption *versus* time are given in *Figure 6* for three copolymerizations with 25, 46, and 56 molar proportions of LIMA in the feed. Kinetics results are collected in *Table 2*, expressed in terms of polymerization rate (R_{po}) and instantaneous copolymer composition (F_{Mo}) *versus* monomer feed composition (f_{Mo}).

From these kinetic data, reactivity ratios were determined according to three conventional methods as given in *Table 2*. An average set of values can be deduced such as: $r_s = 1.23 \pm 0.09$ and $r_{LIMA} = 0.86 \pm 0.1$ which is indicative that a slight composition drift occurs during copolymerization of comonomer mixtures. The value for LIMA, smaller than one, suggests that this monomer is less reactive than styrene, the steric hindrance conferred by the saccharidic moiety favoring cross-propagation. The reverse is true with many other styrene derivatives for which the relative reactivity towards the polystyryl radical is much higher, especially when the substituent is electron donating.

Using the initial comonomer compositions and reactivity ratios, the instantaneous copolymer compositions were calculated from the copolymerization equation and compared to the experimental compositions as reported in *Table 2*: the agreement is good enough to validate the reactivity ratios obtained.

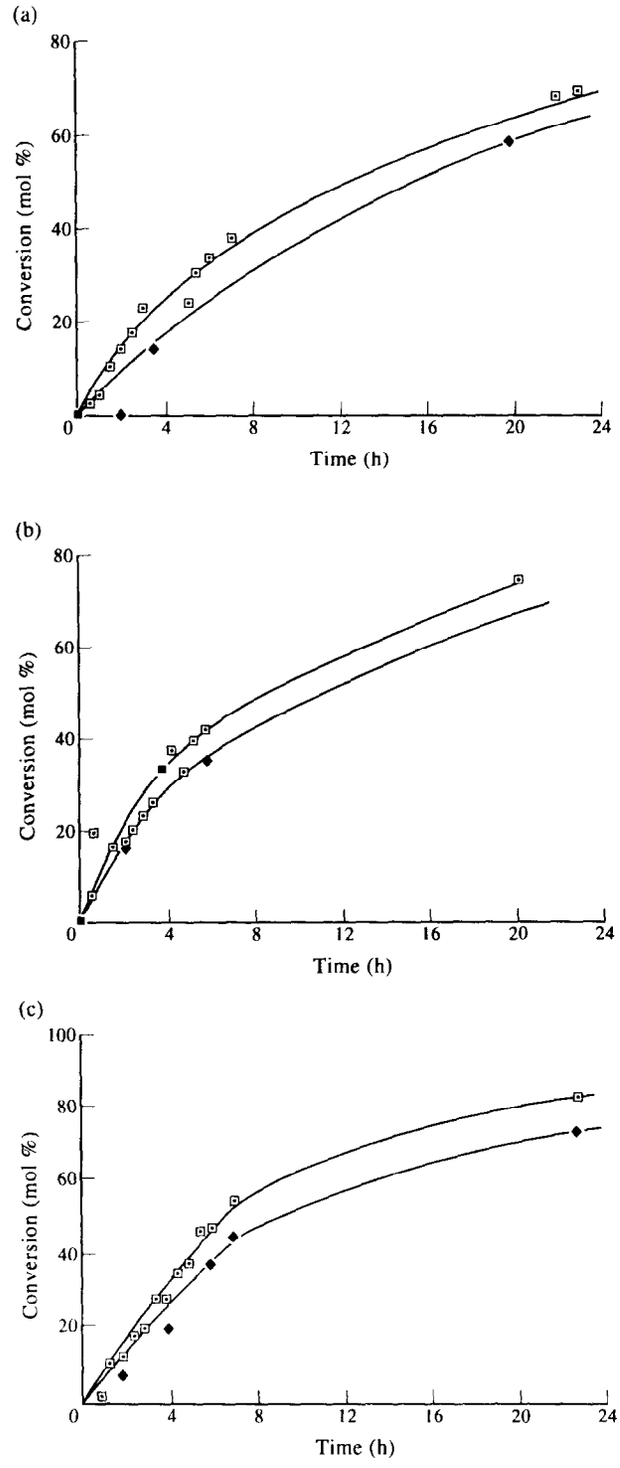

Figure 6 Conversion *versus* time curves for LIMA–styrene copolymerization in DMSO-d_6. Styrene: (□); LIMA: (◆). (a) Copo 5: $f_{Mo} = 0.25$; (b) Copo 6: $f_{Mo} = 0.465$; (c) Copo 7: $f_{Mo} = 0.566$.

Characterization of LIMA containing (co)polymers

Homopoly(LIMA) and copolymers with styrene were characterized with respect to average compositions and molecular weights.

Homopoly(LIMA) was first analysed by performing ^{1}H and ^{13}C n.m.r. in DMSO-d_6 solutions. As shown in *Figure 7*, the ^{1}H n.m.r. spectrum displays all resonance structures corresponding, respectively, to the amide protons (7.4–8.2 ppm), the aromatic protons (6.2–7.0 ppm), the protons of the saccharidic moiety (3.2–3.7 ppm) and

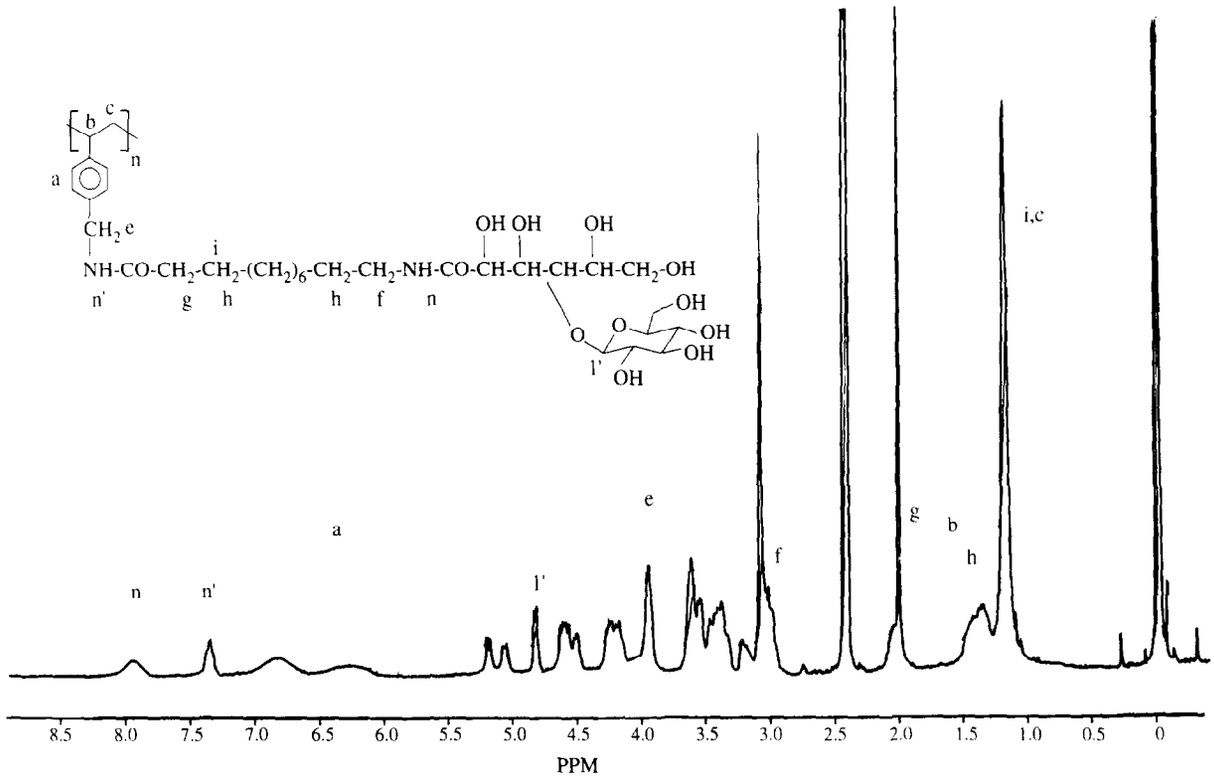

Figure 7 ^{1}H n.m.r. spectrum (200 MHz) of homopoly(LIMA) in DMSO-d_6

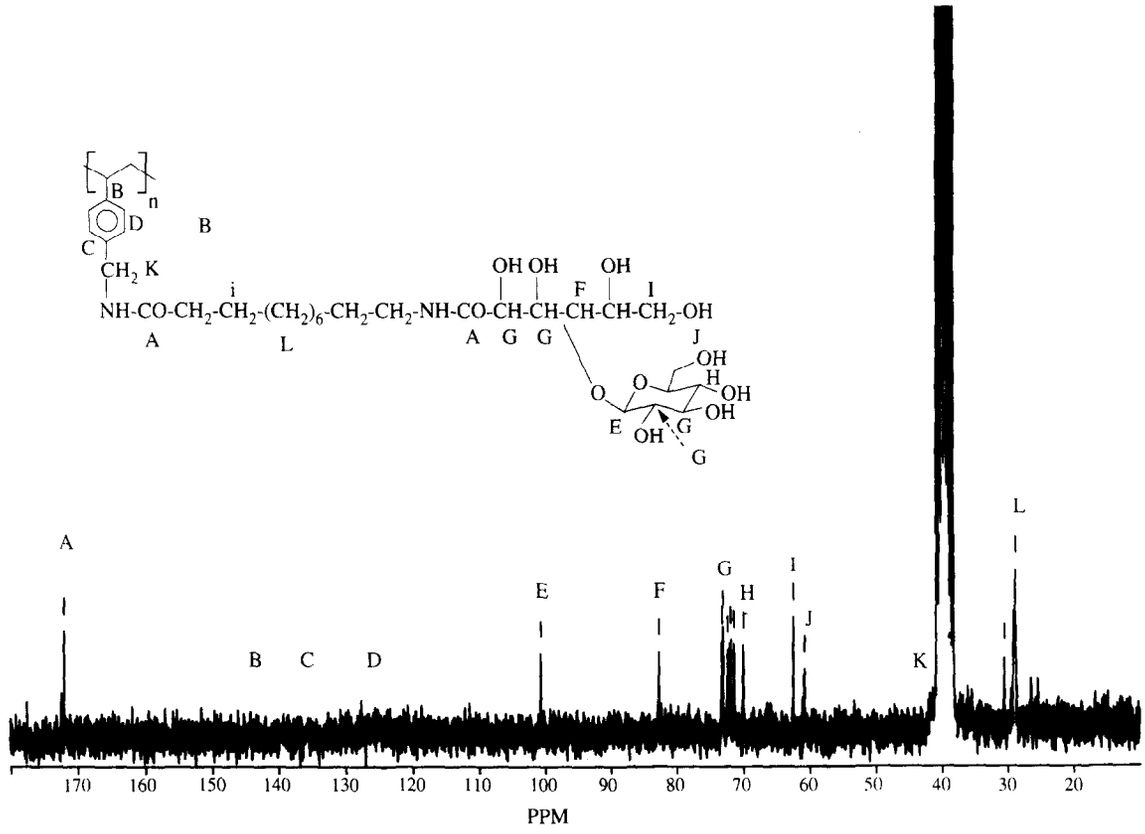

Figure 8 ^{13}C n.m.r. spectrum (50.3 MHz) of homopoly(LIMA) in DMSO-d_6

the methynic and methylenic protons (1.10–1.4 ppm). Interestingly, it was noted that all aromatic protons disappeared when the spectrum was recorded in D_2O solution. Such behavior might be interpreted by considering that these polyamphiphiles would form aggregates in aqueous phase (due to the amphipatic structure of LIMA) where hydrophobic parts would be located in the interior; this would cause a strong decrease of the

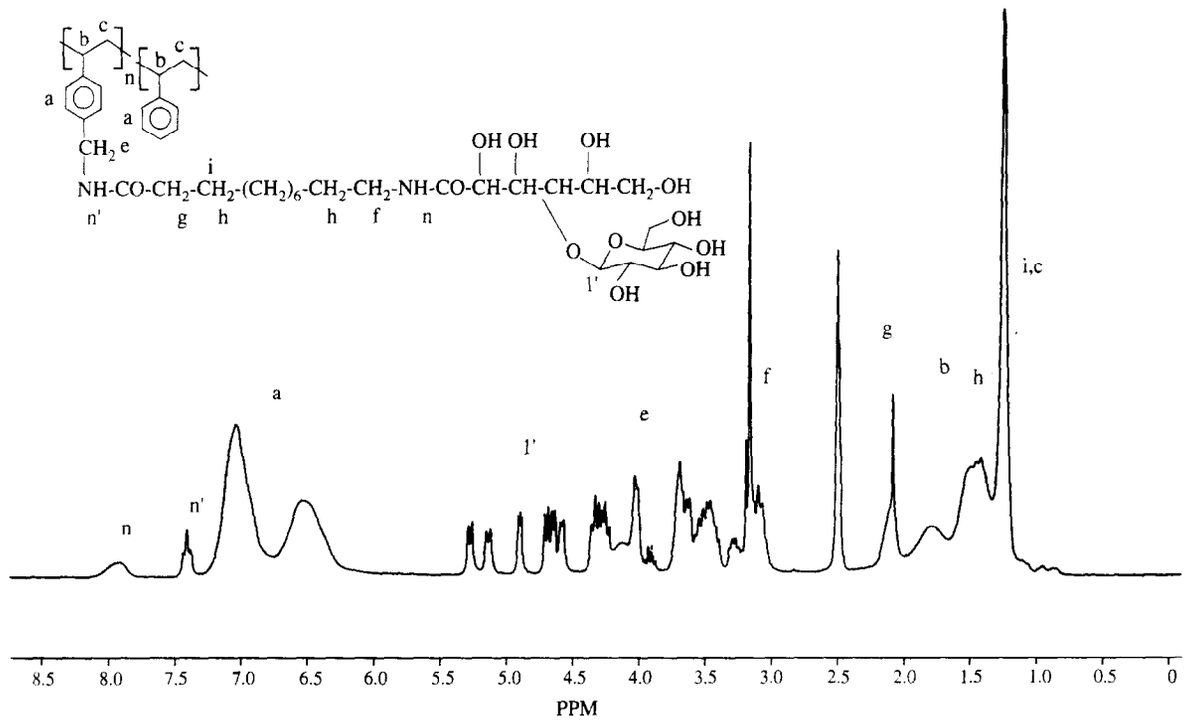

Figure 9 ^{1}H n.m.r. spectrum (200 MHz) of Copo 7 (52.5 mol% LIMA) in DMSO-d_6

alkyl chain mobility resulting in a drastic broadening of the aromatic rays.

As shown in *Figure 8*, the ^{13}C n.m.r. spectrum of poly(LIMA) also exhibits the main features due to the different resonance carbon structures of the macromolecule. However, it was not possible to observe any splitting in the quaternary aromatic structures which could have reflected the expected tacticity effect. Such a phenomenon can be explained by the differences in mobility between the long alkyl chain (giving very intense and thin peaks) and the backbone chain (for which broader peaks are observed).

The copolymer composition was determined both by ^{1}H n.m.r. and elemental analyses. *Figure 9* provides a general view of the n.m.r. spectrum showing all the resonance structures typical of the copolymer. Based on the assignment of aromatic and hydroxyl protons, the molar fraction of LIMA in the various copolymers was determined according to the formula established in the Experimental section. The values obtained are reported in *Table 3* together with those deduced from elemental analysis. A relatively good agreement is observed as well as with the theoretical values obtained from a numerical simulation of the copolymerization equation taking into account the conversion and reactivity ratios of the binary system.

It was also attempted to characterize the molecular weights (MW) and distributions of the various LIMA-containing polymers using g.p.c. in DMF on heating conditions (65°C). The results are summarized in *Table 4* together with that of polystyrene and LIMA monomer. It is worth observing that all copolymers exhibit higher MW than polystyrene, although they were prepared under similar conditions. It should be mentioned that these MW data are apparent since they are related to PS standards; in addition, it should be noticed that LIMA shows an apparent molecular weight much higher than the actual molecular weight and that poly(LIMA) could not be analysed because of its poor solubility in DMF. Such a difference might result from particular interaction between the saccharidic copolymer and the beads filling the columns. Concerning the polydispersity index, the reported values do not deviate too much from the expected values, assuming that termination is mainly by coupling and that MWD broadening did not occur even at high conversion.

Table 3 Reactivity ratios for free-radical copolymerization of LIMA (r_m) with styrene (r_s)

Reactivity ratio	Fineman–Ross	Kelen–Tudös	Tidwell–Mortimer
Styrene (r_s)	1.13	1.32	1.25
LIMA (r_m)	0.74	0.94	0.91

Average values: $r_s = 1.23 \pm 0.09$; $r_m = 0.86 \pm 0.1$

Table 4 Average copolymer compositions of styrene–LIMA copolymers. Comparison with theoretical values

Sample code	Conversion (wt%)	Molar fraction in ^{1}H n.m.r.	Copolymer elemental analysis	Theoretical [a]
EC5	69.8	0.204	0.249	0.231
EC6	75.3	0.394	0.419	0.444
EC7	76.6	0.525	0.534	0.546

[a] With $r_m = 0.86$ and $r_s = 1.23$

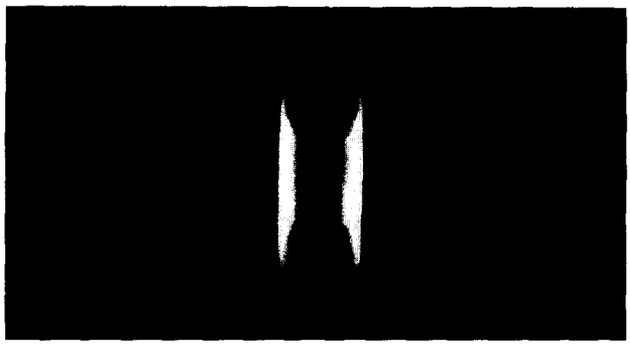

Figure 10 X-ray diagram of copolymer sample (Copo 6) with 42 mol% LIMA

Table 5 Molecular weight and distribution in styrene–LIMA copolymers from g.p.c. analysis

Sample code	M_n	M_w	I_p
Polystyrene	84000	10470	1.25
LIMA	7060	7220	1.02
Copo 5	61300	10400	1.76
Copo 6	68800	155000	2.33
Copo 7	57000	106800	1.94

Table 6 Parameters used to calculate d_A, d_B and S

	V_A ($cm^3\ g^{-1}$)	V_B ($cm^3\ g^{-1}$)	X_A	M_B
pLIMA	0.635	0.975	0.543	300
Copo 5	0.635	0.965	0.367	152.8
Copo 6	0.635	0.969	0.445	186.1
Copo 7	0.635	0.971	0.477	208.7
Copo 2	0.635	0.974	0.531	275.3

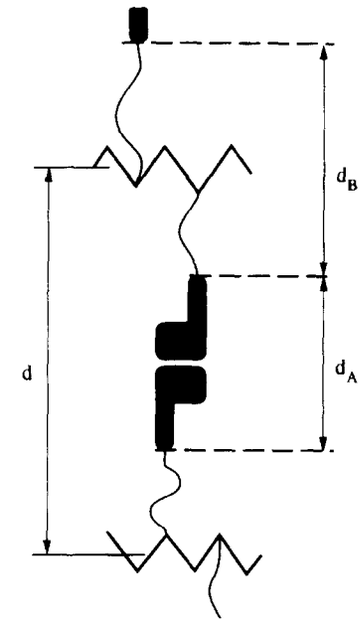

Figure 11 Schematic representation of the lamellar structure in homopoly(LIMA)

Table 7 Structural parameters of poly(LIMA) and (styrene–LIMA)-copolymers

Parameter	pLIMA	Copo 2	Copo 7	Copo 6	Copo5
d (Å)	40.0	41.6	46.6	48.0	48.8
d_A (Å)	17.0	17.6	17.4	16.6	13.5
d_B (Å)	23.0	24.0	29.2	31.4	35.3
S (Å^2)	44.2	42.7	43.2	45.2	55.6
L (Å)	30.0				
L_A (Å)	8.5				
LIMA (mol%)	100	87.4	53.4	41.9	24.9

Liquid crystal properties

The structure of the LIMA monomer and comb-like homopoly(LIMA) and copolymers of LIMA and styrene were studied, by X-ray diffraction, between room temperature and the clearing or decomposition temperature.

Description of the X-ray diagrams. All obtained X-ray diagrams exhibit in the low-angle region a set of 1–3 sharp lines with reciprocal spacings in the ratio 1, 2, 3 characteristic of a lamellar structure (*Figure 10*), but they differ by the aspect of the wide-angle domain. For the monomer LIMA at temperatures lower than 157°C, they show sharp reflections characteristic of a crystalline structure. For LIMA, at temperatures between 157°C and the clearing temperature and for the homo and copolymers at temperatures lower than the clearing temperature, they display in the wide-angle region a diffuse band characteristic of liquid-like paraffinic chains[44]. Using the liquid-crystal classification the lamellar structure is a Smectic A structure characterized by the absence of periodic order in the plane of the lamellae[45].

Structure of the homopolymer of LIMA. The repeating unit of the comb-like polymer corresponds to the following general formula:

$H_2C\text{-}CH\text{-}C_6H_4\text{-}CH_2\text{-}NH\text{-}CO\text{-}(CH_2)_{10}\text{-}$Maltonamide

Such a repeating unit consists of two parts: a hydrophilic part, A, of molecular weight $M_A = 356$ corresponding to the maltonamide, and a hydrophobic part, B, of molecular weight M_B (*Table 6*) corresponding to the lipidic chains: $(CH_2)_n$ and the main chain unit: $H_2C\text{-}CH\text{-}C_6H_4\text{-}CH_2\text{-}NH\text{-}CO$-. The two parts of the repeating unit of the comb-like polymers are incompatible and give rise to a microphase separation at the molecular level. The lamellar mesomorphic structure can be described as follows.

The lamellar structure (Smectic A) consists of plane, parallel, equidistant sheets: each sheet, of thickness d, results from the superposition of two layers; one, of thickness d_A, contains the hydrophilic maltonamide units, while the other, of thickness d_B, contains the polymer main chain and the lipidic side chains (*Figure 11*).

The total thickness d of a sheet is obtained directly from the X-ray patterns. The other parameters: d_A, d_B and S (the average surface area occupied by a repeating unit at the interface between the hydrophilic and hydrophobic layers) are obtained using the following formulae based on simple geometrical considerations:

$$d_B = d[1 + X_A V_A/(1 - X_A)V_B]^{-1} \quad (1)$$

$$d_A = d - d_B \quad (2)$$

$$S = 2M_A V_A/Nd_A \quad (3)$$

where X_A is the weight fraction of the hydrophilic moiety A (*Table 6*), V_A is the specific volume of the hydrophilic moiety A (*Table 6*), V_B is the specific volume of the hydrophobic moiety B (*Table 6*), and M_A is the molecular mass (356) of the hydrophobic moiety. V_A and V_B are calculated using the values of the volumes of the different chemical groups of the A and B moieties[46].

The values of the geometrical parameters of the lamellar structure are given in *Table 7*. The value of S found for the dry homopolymer (44.2 Å^2) confirms the liquid-like character of the paraffinic chains.

With a view to obtaining information on the respective organization of the hydrophilic and hydrophobic parts of the molecules, CPK models of the repeating unit of the polymer were built and the maximum total length L (the paraffinic chains are in an all-*trans* conformation) and the length L_A of the hydrophilic moiety were measured (*Table 7*).

For homopoly(LIMA), the molecular models showed that the glucose residue of the saccharidic moiety is perpendicular to the average direction of the side chain (*Figure 12*), and that $d_A = 2L_A$ (*Table 7*). Therefore, in the lamellar structure of poly(LIMA), the saccharidic chains form a double layer with the glucose residues of two opposite side chains roughly parallel in order to obtain a maximum of interactions, while the hydrophobic chains in a liquid-like conformation also form a double layer; so the lamellar structure of poly(LIMA) belongs to the Smectic A2 type. This structure is in agreement with the structure found for the LIMA molecule in the conformation of minimal energy using a logiciel PCMODEL and the HSEA (Hard Sphere Exo Anomeric) approach.

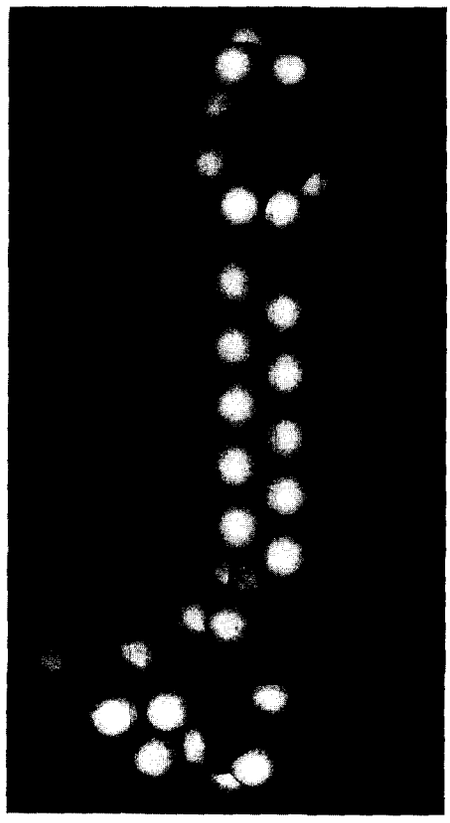

Figure 12 Molecular model (CPK) of homopoly(LIMA)

Structure of the copolymers. For the copolymers, the hydrophilic moiety A is identical to that of the homopolymer but the hydrophobic moiety contains the hydrophobic part of LIMA and styrene (S) and its molecular weight is: $M_B = (1-x)M_{(S)} + xM_{B(LIMA)}$, where x is the mole fraction of LIMA in the copolymer.

Thus, the lamellar structure of the copolymers is similar to that of the homopolymer except that the hydrophobic layer contains both styrene and the hydrophobic moiety of LIMA.

The values of d_A, d_B and S can be calculated by equations (1)–(3) taking into account the new values of X_A and V_B (given in *Table 6*). The values obtained are given in *Table 7* and plotted as a function of the styrene content of the copolymers in *Figure 13*.

One can see on *Figure 13* that when the styrene content of the copolymer increases, the total thickness d of a sheet and the thickness d_B of the hydrophobic layer both increase, while the thickness d_A of the hydrophilic layer and the surface S at the interface between the hydrophilic and hydrophobic layers remain constant until a styrene content of about 60%. For higher styrene contents, d_A slightly decreases while S increases. This behavior is in agreement with the phase separation between the hydrophilic and hydrophobic domains, the styrene swelling the hydrophobic domains without disturbing the hydrophilic domains until its concentration becomes too high and begins to perturb the lamellar order as revealed by the decrease of the sharpness of the low-angle reflection on X-ray diagrams.

Structure of LIMA monomer. LIMA alone exhibits 2 phases as a function of temperature: a crystalline phase until 157°C and a mesophase between 157°C and 178°C.

The mesophase is characterized by a lamellar thickness $d = 40.9$ Å similar to that of the homopolymer (see *Table 7*). Therefore, one can deduce that this structure is a double-layer smectic structure SA2, with layer thicknesses of the hydrophilic and hydrophobic layers $d_A = 23.5$ Å and $d_B = 17.4$ Å calculated using equations (1) and (2). In the crystalline structure, the lipidic chains are crystallized and one could think of a double-layer tilted structure; but a tilt angle F, given by $\cos\Phi = d/2L$, would be very important: $\Phi = 39°$. Another possible structure would be an orthogonal one with a partial interdigitation (at the level of the styrene ring). Such a structure would be stabilized not only by interactions

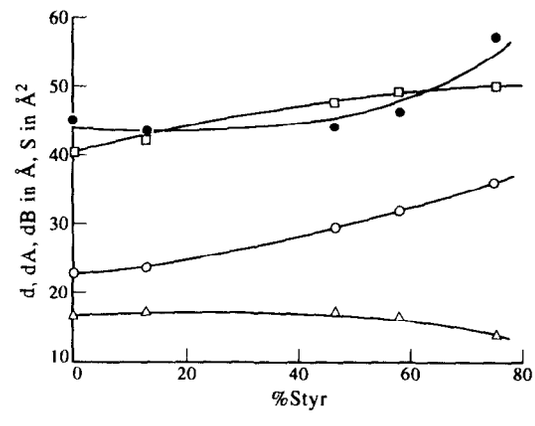

Figure 13 Variation of structural parameters (d (□), d_A (△), d_B (○), S (●)) with molar composition in styrene–LIMA copolymers

between the glucose residues of the saccharidic moiety (as in the mesophase), but by interactions between the aromatic rings.

CONCLUSIONS

A new amphiphilic monomer, 11-(*N*-*p*-vinylbenzyl)amidoundecanoyl maltobionamide (LIMA) bearing a saccharidic moiety as the hydrophilic part, was synthesized via a five-step procedure providing a satisfactory yield. It was fully characterized with regard first, to molecular structure by ^{1}H and ^{13}C n.m.r. spectroscopy, and second, to its amphiphilic behavior by determining the critical micelle concentration in water ($1.2\,mol\,l^{-1}$) owing to surface tension and fluorescence measurements.

Kinetics of radical-initiated polymerization of LIMA in DMSO-d_6 solution allowed the estimation of a $k_p/k_t^{1/2}$ value of 0.17 which is indicative that this monomer homopolymerized much more rapidly than various styrene-terminated monomers. Copolymerizations with styrene were also performed and the reactivity ratios obtained ($r_M = 0.86$ and $r_S = 1.23$) suggested that copolymers with a fairly compositional homogeneity could be produced.

Copolymer compositions were determined both by elemental and n.m.r. analyses and a good agreement was exhibited with the theoretical compositions, which validated the values of the reactivity ratios; however, no detailed information could be obtained on the microstructure, especially the monomer sequence distribution. Owing to X-ray analysis, these resulting comb-like (co)polymers were found to show liquid crystal properties with a smectic A lamellar structure. This allowed us to provide information on the various parameters describing the molecular organization of the hydrophobic and hydrophilic parts of LIMA. In the case of styrene copolymers, the overall thickness of the lamellae and that of the hydrophobic layer increased upon increasing the styrene content in the copolymer, whereas the hydrophilic layer almost remained constant except for too high a styrene content.

Additional work is currently underway in order to better characterize the physicochemical properties of these carbohydrate-containing copolymers in solution with a view to investigating their performances for grafting biologically-active molecules. Moreover, the outstanding properties of LIMA were exploited for modifying the surface morphology of polystyrene latex particles[47] via emulsion copolymerization in the presence of styrene. The corresponding functionalized supports bearing sugar moieties were found suitable for studying interactions with model proteins[48].

REFERENCES

1 Kobayashi, K., Aoki, K., Sumitomo, H. and Akaike, T. *Makromol. Chem., Rapid Commun.* 1990, **11**, 577
2 European Patent Application 0 394 068 A1, 1990
3 Kobayashi, K., Sumitomo, H. and Ina, Y. *Polym. J.* 1985, **17**, 567
4 Kobayashi, A., Akaike, T., Kobayashi, K. and Sumitomo, H. *Makromol. Chem., Rapid Commun.* 1986, **7**, 645
5 Kugumiya, T., Yagawa, A., Maeda, A., Nomoto, H., Tobe, S., Kobayashi, K., Matsuda, T., Onishi, T. and Akaike, T. *J. Bioactive Compatible Polym.* 1992, **7**, 337
6 Nakaya, T., Nishio, K., Memita, M. and Imoto, M. *Makromol. Chem., Rapid Commun.* 1993, **14**, 77
7 Kochetkov, N. K. *Pure Appl. Chem.* 1984, **56**, 923
8 Duncan, R., Kopeckova-Rejmanova, P., Strohalm, J., Hume, I., Cable, H. C., Pohl, I., Lloyd, J. B. and Kopecek, J. *Br. J. Cancer* 1987, **55**, 165
9 Rozalski, A., Brade, L., Kunh, H. M., Brade, J., Kosma, P., Appelmk, B. J., Kusumoto, S. and Paulsen, H. *Carbohydr. Res.* 1989, **193**, 257
10 Koyama, Y., Yoshida, A. and Kurita, K. *Polym. J.* 1986, **18**, 479
11 Ziegast, G. and Pfannemüller, B. *Carbohydr. Res.* 1987, **160**, 185
12 Klein, K. A. and Begli, A. H. *Makromol. Chem.* 1989, **190**, 2527
13 Roy, R. and Tropper, F. *J. Chem. Soc., Chem. Commun.* 1988, 1058
14 Nishimura, S., Matsuoka, K., Furuike, T., Ishi, S., Kurita, K. and Nishimura, K. *Macromolecules* 1991, **24**, 4236
15 Klein, K., Kunz, M. and Kowalczyk, J. *Makromol. Chem.* 1990, **191**, 517
16 Gallot, B. and Marchin, B. *Liquid Crystals* 1989, **5**, 1729
17 Nakaya, T., Memita, M. and Kang, M. *Macromol. Rep.* 1993, **A30(5)**, 349
18 Pfannemüller, B. *Starch/Stärke* 1988, **40**, 476
19 Charreyre, M. T., Boullanger, P., Pichot, C., Delair, T., Mandrand, B. and Llauro, M. F. *Makromol. Chem.* **194**, 117 (1993)
20 Gallot, B., Revilla, J., Charreyre, M. T. and Pichot, C. in 'Liquid Cristalline Polymers' (Ed. C. Carfagna), Pergamon, Oxford 1994, p. 1
21 Charreyre, M. T., Boullanger, P., Delair, T., Mandrand, B. and Pichot, C. *Colloid. Polym. Sci.* 1993, **271**, 668
22 Demharter, S., Richtering, W. and Mulhaupt, R. *Polym. Bull.* 1995, **34**, 271
23 Kando, S., Ohtsuka, T., Ogura, K. and Tsuda, K. *J. Macromol. Sci. Chem.* 1979, **A13**, 767
24 Kobayashi, K., Sumitomo, H. and Ina, Y. *Polym. J.* 1983, **15**, 667
25 Fineman, M. and Ross, D. *J. Polym. Sci.* 1950, **5**, 259
26 Kelen, T. and Tüdös, F. *J. Macromol. Sci., Chem.* 1975, **A9**, 1
27 Tidwell, P. W. and Mortimer, G. A. *J. Polym. Sci.* 1965, **3**, 369
28 Moroder, L., Hallet, A., Wünsch, E., Keller, O., Wersin, G. and Hoppe-Seyler, Z. *Physiol. Chem.* 1976, **357**, 1651
29 Perseo, G., Piani, S. and de Castiglione, R. *Int. J. Peptide Protein Res.* 1983, **21**, 227
30 Paquet, A. *Can. J. Chem.* 1976, **54**, 733
31 Kalyanasundaram, K. and Thomas, J. K. *J. Am. Chem. Soc.* 1977, **99**, 2039
32 Turro, N. J., Grätzel, M. and Braun, A. M. *Angew. Chem., Int. Ed. Engl.* 1980, **19**, 675
33 Zhao, C. L. and Winnik, M. A. *Langmuir* 1990, **6**, 514
34 Wilhelm, M., Zhao, C. L., Wang, Y., Xu, R., Winnik, M. A., Mura, J. L., Riess, G. and Croucher, M. D. *Macromolecules* 1991, **24**, 1033
35 Rempp, P. and Merrill, E. W. in 'Polymer Synthesis', Hüthig and Wepf, Basel, 1986
36 Kulkarni, M. G., Mashellkar, R. A. and Doraiswamy, L. K. *J. Polym. Sci., Polym. Lett. Edn.* 1979, **17**, 713
37 Charleux, B., Pichot, C. and Llauro, M. F. *Polymer* 1993, **34**, 4352
38 Charreyre, M. C., Razafindrakoto, V., Veron, L., Delair, T. and Pichot, C. *Makromol. Chem.* 1993, **195**, 2141
39 Schulz, G. V., Henrici-Olivé, G. and Olivé, S. *Z. Phys. Chem.* 1960, **27**, 1
40 Yokota, K., Kani, M. and Ishii, Y. *J. Polym. Sci. A-1* 1968, **6**, 1325
41 Burnett, G. M., Evans, P. and Melville, M. W. *Trans. Faraday Soc.* 1953, **49**, 1105
42 Platé, N. A. and Ponomarenko, A. G. *Polym. Sci. USSR* 1974, **16**, 3067
43 Davis, T. P. and O'Driscoll, K. F. *Macromolecules* 1990, **23**, 2113
44 Luzzati, V., Mustacchi, H., Skoulios, A. and Husson, F. *Acta. Crystallogr.* 1960, **13**, 660
45 De Vries, A. *Mol. Cryst. Liq. Cryst.* 1985, **131**, 125
46 Gabani, S., Gianni, P., Molica, P. and Lepori, L. *J. Solution Chem.* 1983, **10**, 563
47 Revilla, J., Elaissari, A., Pichot, C. and Gallot, B. *Polym. Adv. Tech.* 1995, **6**, 455
48 Elaissari, A., Revilla, J., Carrière, P. and Pichot, C. submitted for publication